

## Field Emission Studies of the sub-micron sized rare earth hexaborides (NdB<sub>6</sub>, CeB<sub>6</sub>, EuB<sub>6</sub>) Crystals

Shagufta Parveen M.A<sup>1</sup>, Altaf Inamdar<sup>2</sup>  
<sup>1,2</sup>(Applied Sciences, MMANTC, India)

**Abstract:** Rare earth hexaborides are a family of compounds which have low work function, high melting point and high mechanical strength. These properties are highly suitable for cold cathode applications. Therefore in present work I have studied the field emission (FE) properties of different rare earth hexaborides (RB<sub>6</sub>: CeB<sub>6</sub>, NdB<sub>6</sub> and EuB<sub>6</sub>) at the base pressure of  $1 \times 10^{-8}$  mbar. The structural, compositional and morphological analysis of the prepared cathode NdB<sub>6</sub>, CeB<sub>6</sub> and EuB<sub>6</sub> have been carried out using scanning electron microscope (SEM), X-ray diffraction (XRD). The observations regarding the experiment are tabulated and comparative conclusions are made based on observations.

**Keywords:** Cold cathode, Field Emission, Hexaborides, Rare earth, Work Function.

### I. Introduction

Rare earth metal hexaboride (RB<sub>6</sub>) have gain the importance due to its set of Physico-chemical properties such as low work function, high melting point, low vapour pressure, low sputtering coefficient for being an ideal cold cathode. [1,2,3] Cold cathodes are essential elements in a variety of applications such as miniature X-ray sources, flat panel display and cathode-ray tube monitors. Electron source can be produced from the suitable cathode materials either via thermionic emission or via field emission. Mainly, as compared to thermionic emission, field emission based devices/cathodes typically attracts more attention due to the relaxation in the operating voltage range, low temperature range (ideally 0 K), good emission current stability, longevity, high brightness, large area, reduced device size, and low sputtering coefficient of the materials. In principally, the field emission current density exponentially depends on the work function ( $\phi$ ) of the emitter and applied electric field ( $E$ ) as *via* the Fowler-Nordheim (F-N) equation. Fortunately rare earth metal hexaborides having lower work function ( $\phi$ ) in the range of 1.5- 3 eV [4, 5] in contrast to metals having  $\phi$  is usually in the range of 4 to 7 eV. For such high  $\phi$  material electron emission occurs at large applied electric field (typically the order of  $10^9$  V/m), which can also induce the vacuum breakdown and high electrical discharge. From a practical application point of view, the key issues are relaxation in operating voltage; very higher emission current density and stable emission current, longevity of the cathode are mostly required. As the turn-on or threshold field values are dependent on the 'extrinsic' (shape and size) forms of the emitter, and its intrinsic properties, such as work function, mechanical strength etc. Therefore there is a scope, to obtain a higher FE field emission performance from low work function materials, RB<sub>6</sub> based nanostructures. In the present study, we have investigated FE study of commercially available RB<sub>6</sub> microstructures.

### II. Experimental Section

#### 1. Materials:

Microcrystals of RB<sub>6</sub> were purchased from Alfa aesar (purity 99.998 %) was used for further characterization.

#### 2. Field Emission Characteristics:

The field emission current density (J) versus applied electric field (E) and emission current (I) versus time (t) characteristics were measured in a planar 'diode' configuration at base pressure of  $\sim 1 \times 10^{-8}$  mbar. In a typical 'diode' configuration there is phosphor coated semitransparent screen (a circular disc of diameter  $\sim 40$  mm) as an anode. In order to investigate the FE, very small quantity of RB<sub>6</sub> (EuB<sub>6</sub>, CeB<sub>6</sub>, EuB<sub>6</sub>) powder was sprinkled onto a rounded piece of carbon tape (radius  $\sim 2.5$  mm), which was then mounted in the parallel plate diode assembly. The cathode (RB<sub>6</sub> micro sheets coated carbon tape) was held parallel with an anode screen in close proximity. The ultra-high vacuum chamber is equipped with rotary backed turbo molecular pump, sputter ion pump and titanium sublimation pump. For achieving base pressure of  $\sim 1 \times 10^{-8}$  mbar, the chamber is baked at 200°C for 12 hrs. During FE measurements cathode-anode separation was fixed ( $\sim 1$  mm). We measured emission current on Keithely Electrometer (6514) by sweeping dc voltage applied to cathode with a step of 40 V (0-40 kV, Spellman, U.S.). The field emission current stability is investigated using computer controlled data acquisition system with sampling interval of 10s. In order to avoid any leakage current special care was taken by using shielded cables and ensuring proper grounding. Before recording the FE measurements, pre-conditioning

of the cathode was carried out by keeping it at ~ 2 kV so as to remove the loosely bound particles and/or contaminants by residual gas ion bombardment. Increasing the cathode voltage carefully the field emission image was observed on the screen. The photographs were recorded with a digital camera (model: NIKONE8700).

### III. Result and Discussion

#### 1. SEM:

The surface morphology of the purchased RB<sub>6</sub> powder was characterized under SEM as shown in Figure 1. The SEM images of RB<sub>6</sub> shows the irregular shaped particulates, with micron size cubes excludes GdB<sub>6</sub> cover the entire cathode surface. The SEM images of GdB<sub>6</sub> shows that granular particulates with average particle size ~100 nm.

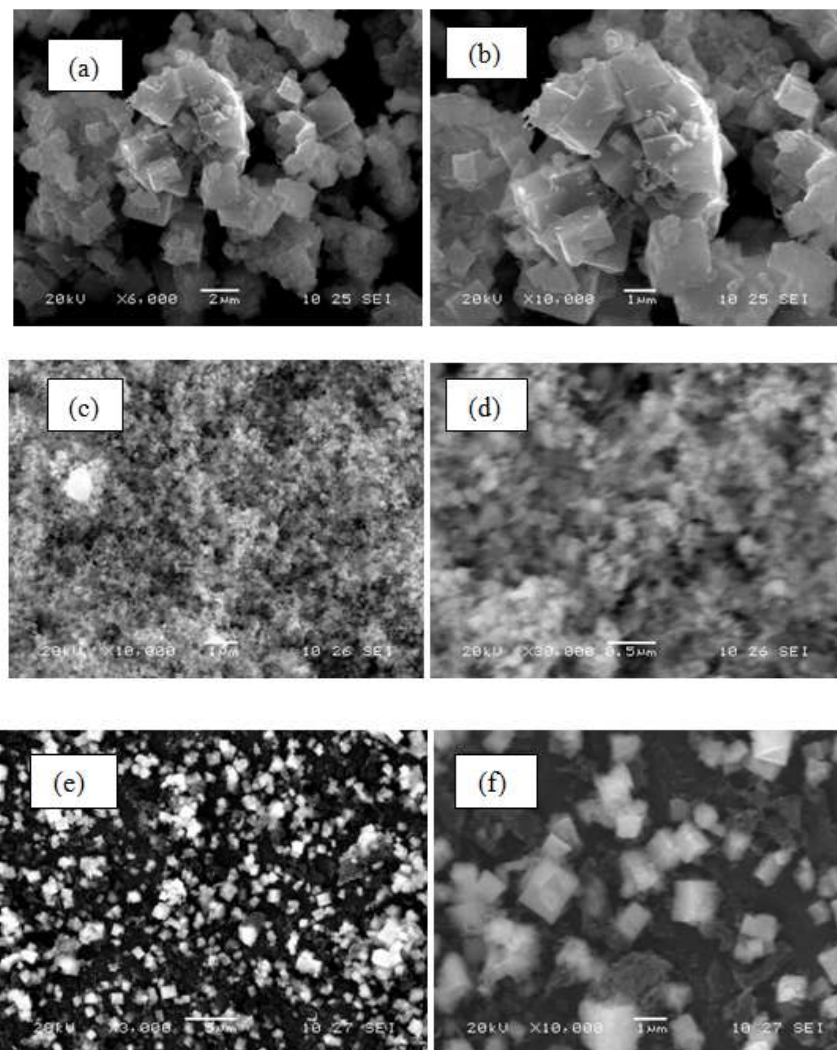


**Figure1:** (a),(b) The SEM of NdB<sub>6</sub> (c),(d) The SEM of CeB<sub>6</sub> (e),(f) The SEM of EuB<sub>6</sub>

#### 2. X-Ray diffraction studies:

The crystalline nature of the purchased RB<sub>6</sub> powder was analyzed by X-ray diffractometer as shown in given Figure 2. A typical XRD patterns exhibit a set of well-defined diffraction peaks indexed to crystalline cubic phase of RB<sub>6</sub>. No characteristic diffraction peaks due to other crystalline phases were observed, indicating good purity of the purchased products.

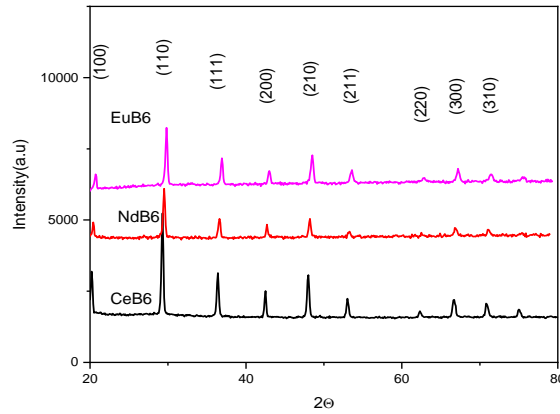


**Figure 2:** A typical XRD pattern of RB<sub>6</sub> (EuB<sub>6</sub>,NdB<sub>6</sub>,CeB<sub>6</sub>)

### 3. FEM Studies:

Figures 3.1,3.2,3.3(a) depicts plots of the emission current density (J) versus applied electric field (E) of RB<sub>6</sub> emitters. The values of turn-on and threshold field, corresponding to emission current density of ~1 μA/cm<sup>2</sup> and ~100 μA/cm<sup>2</sup>, are tabulated in given table for different RB<sub>6</sub>. As the applied voltage is increased further, the emission current is found to increase rapidly and very high emission current density was increases for RB<sub>6</sub> emitter. The observation of lower values of turn-on and threshold fields, and extraction of very high emission current density at relatively lower applied electric field, is attributed to the high aspect ratio and low work function of RB<sub>6</sub>.

The emission characteristic of large area planar emitters is explained by modified Folwer-Nordheim equation stated as,

$$J = \lambda_M a \phi^{-1} E^2 \beta^2 \exp\left(-\frac{b \phi^{\frac{3}{2}}}{\beta E} v_F\right)$$

Where J is the emission current density, E is the applied average electric field, a and b are constants, typically  $1.54 \times 10^{-10}$  (AV<sup>-2</sup>eV) and  $6.83 \times 10^3$  (VeV<sup>-3/2</sup>μm<sup>-1</sup>), respectively, φ is the work function of the emitter material, λ<sub>M</sub> a macroscopic pre-exponential correction factor, v<sub>F</sub> is value of the principal Schottky-Nordheim barrier function (a correction factor), and β is the microscopic field enhancement factor. The FE characteristics are further analyzed by plotting a graph of ln (J/E<sup>2</sup>) versus 1/E. This graph is known as F-N plot. Figure 3.1,3.2,3.3(b) depicts the F-N plots of the RB<sub>6</sub> emitters. Usually, the slope of the F-N plot is used to determine the value of field enhancement factor (β).

In the present studies, the values of β are estimated and tabulated in given table for different RB<sub>6</sub>. From device point of view the emission current stability is an important parameter of the emitter. Figures 3.1,3.2,3.3(c) depict long term emission current stability (I-t) of the RB<sub>6</sub> emitters studied at pre-set current values. The emission current exhibits some excursions which are superimposed on 'spike' like fluctuations. The fluctuations are mainly due to various atomic scale processes (migration, adsorption and desorption of the residual gaseous species) on the emitter surface. In case of planar emitter, 'excursions' observed in the emission current are due to many factors like field induced stresses causing variation in field screening amongst closely spaced emission sites, 'extinction' and 'regeneration' of emission sites due to residual ion bombardment, and so on. In addition to these, the 'un-cleaned' nature of cathode may offer noticeable contribution to emission current fluctuations. No doubt that these fluctuations in the emission current can be minimized by properly tuning the morphology (minimizing the field screening effect) and utilizing thoroughly cleaned emitter or providing in-situ cleaning scheme (minimizing the 'spikes' and excursions). Figures 3.1,3.2,3.3(d) depict the typical field emission images of the RB<sub>6</sub> field emitters recorded at the onset of stability measurements. The FE micrographs are comprised of a large number of bright spots indicating the micrometric dimensions of the emission sites.

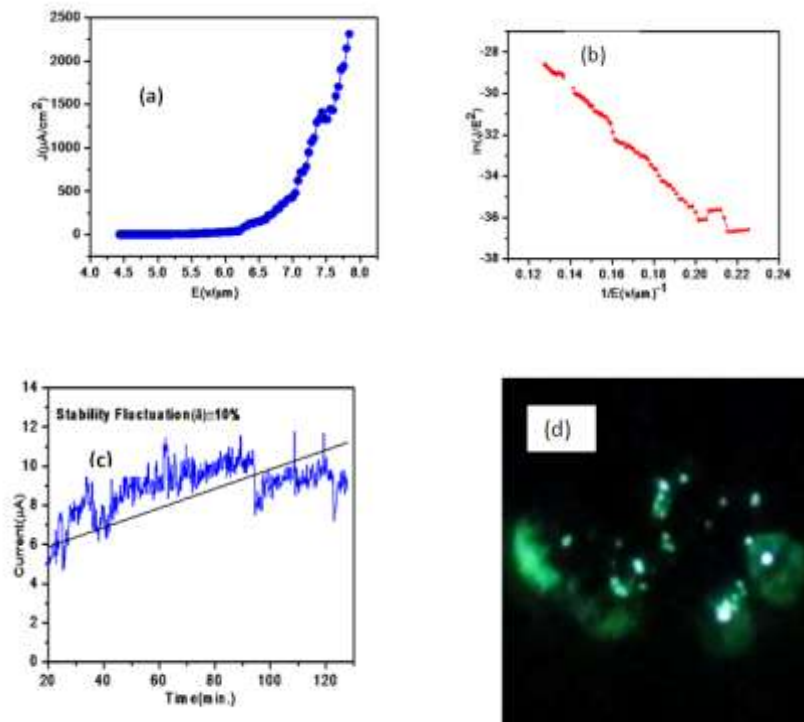


**Figure 3.1:** Field emission characteristics of the  $NdB_6$  emitter (a) emission current density versus applied electric field (J-E) curve (b) F-N plot (c) emission current versus time (I-t) plot with (d) typical field emission micrographs of  $NdB_6$  emitter.

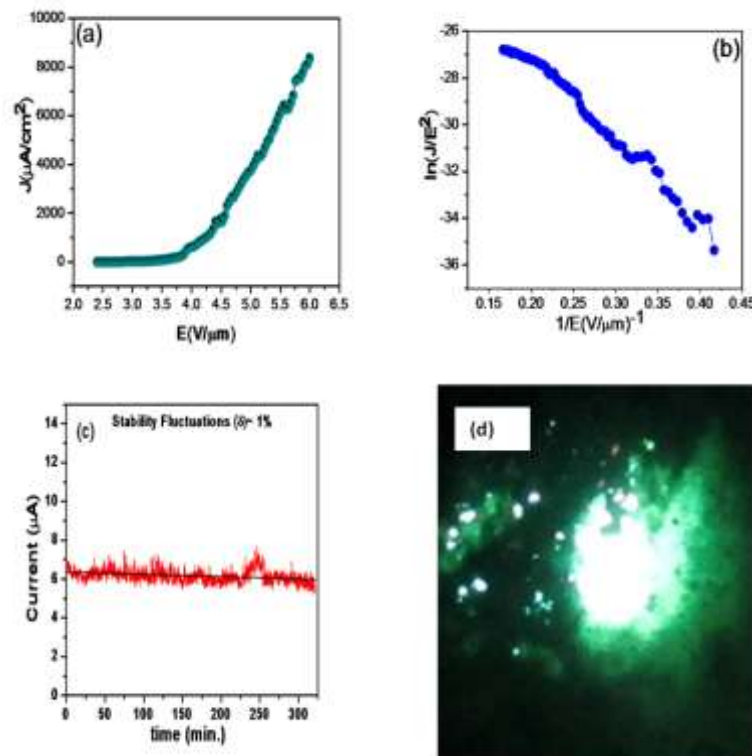


**Figure 3.2:** Field emission characteristics of the  $CeB_6$  emitter (a) emission current density versus applied electric field (J-E) curve (b) F-N plot (c) emission current versus time (I-t) plot with (d) typical field emission micrographs of  $CeB_6$  emitter

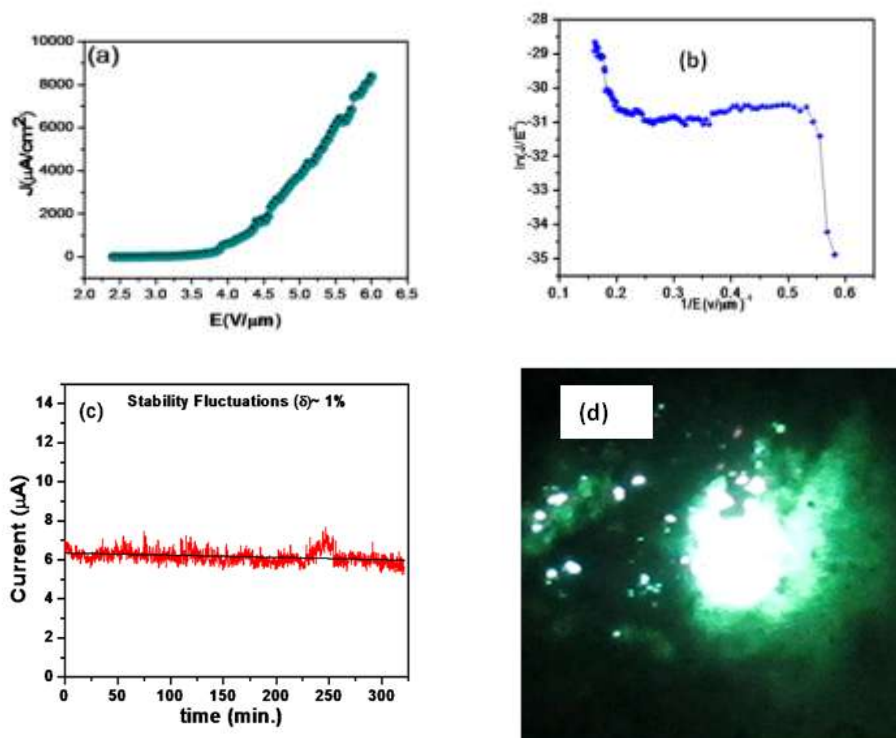


Figure 3.3: Field emission characteristics of the  $EuB_6$  emitter (a) emission current density versus applied electric field (J-E) curve (b) F-N plot (c) emission current versus time (I-t) plot with (d) typical field emission micrographs of  $EuB_6$  emitter.

#### IV. Conclusion

Cathode material	Turn on field for $1\mu A/cm^2$	Threshold field for $10\mu A/cm^2$	Field Enhancement Factor ( $\beta$ )	Stability Fluctuations ( $\delta\%$ )	Stability Time(min.)
$NdB_6$	5.04 V/ $\mu m$	5.6 V/ $\mu m$	149.65	10	350
$CeB_6$	3.16 V/ $\mu m$	3.84 V/ $\mu m$	807.39	1	350
$EuB_6$	2.12 V/ $\mu m$	5.48 V/ $\mu m$	1130.3	51	350

From comparative study we concluded that among these three RB<sub>6</sub>; CeB<sub>6</sub> is best cathode material for commercial application due to low turn on field and higher stability.

#### References

- [1]. S.R Suryawanshi;D.J.Late;M.A.More;A.K.Singh;S.Sinha,3D hetero architecture of  $GdB_6$  nano particles on lessened cubic  $Cu_2O$  nano wires:enhanced field emission behavior, *Proc. Vacuum Nanoelectronics Conference(IVNC)*, 2015, 122-123
- [2]. M.Zhang;Y.Jia;G.Xu;P.Wang;X.Wang;S.Xiong;X.Wang;Y.Qian,Mg-assisted autoclave synthesis of  $RB_6$  submicron cubes and  $SmB_6$  submicron rods,*Eur.J.Inorg.chem.*2010, 1289-1294
- [3]. X.H.Ji,Q.Y.Zhang;J.Q.Xu;Y.M.Zhao,Rare earth hexaborides nano structures:Recent advances in materials,characterization of materials and investigations of physical propertis,*Prog.Solid State Chem.*39(2011) 51-69
- [4]. J.Xu;G.Hou;H.Li;T.Zhai;B.Dong;H.Yan;Y.Wang,B.Yu;Y.Bando;D.Golberg,Excellent field emission performance of Neodymium hexaboride( $NdB_6$ ) nanoneedled with Ultra-low work function,*NPG AsiaMater* 5,53(2013)
- [5]. R.K.Selvan; I.Genish; I.Perelshtein; J.M.CalderonMoreno; A.Gedanken,Single Step low temperature synthesis of Submicron-sized Rare Earth Hexaborides, *J.Phys.Chem.C.* 112(2008) 1795-1802